Chemical and Process Engineering 2022, 43 (2), 229–242
DOI: 10.24425/cpe.2022.140826

Low-cost removal of basic red 9 using cow dung ash

Raj Kumar Arya[1*], Ghanshyam Meena[2,6], Devyani Thapliyal[1], Sanghamitra Barman[3], Gopinath Halder[4], Pooja Shandilya[5]

[1]Dr. B.R. Ambedkar National Institute of Technology, Department of Chemical Engineering, Jalandhar, 144011, Punjab, India

[2]Jaypee University of Engineering and Technology, Guna, 473226, Madhya Pradesh, India

[3]Thapar Institute of Engineering and Technology, Department of Chemical Engineering, Patiala, 147004, Punjab, India

[4]National Institute of Technology Durgapur, Department of Chemical Engineering, M. G. Avenue, Durgapur-713209, West Bengal, India

[5]Shoolini University, School of Advanced Chemical Sciences, Solan HP, 173229, India

[6]National Fertilizers Ltd., Bathinda, Punjab-151003, India

In the present study, basic red 9 had been removed from synthetic waste water using animal waste. Cow dung ash had been prepared and characterized by scanning electron microscope. Morphology analysis shows very fine particles of less than 1 μm. The pH analysis study favours a pH of 8.5 for maximum dye removal. The removal of basic red 9 was very fast on cow dung ash. Percentage dye removal was 80.24% and 95.24 in 5 minutes and 90 minutes, respectively at initial dye concentration of 10 ppm.

Keywords: adsorption isotherms, adsorption kinetics, dye removal, low-cost adsorbent, cow dung ash

1. INTRODUCTION

Adsorption is the most widely used wastewater treatment technique not only because it is extremely effective but also it is eco-friendly, highly-efficient, has simple design, and easy operation. Also, it has been found that it does not generate any hazardous by-products as mentioned by Sivarajasekar and Baskar (2014). The study reported here is first in its kind under low-cost removal of basic red 9. In this work, cow dung ash is being used to remove the basic red 9 from synthetic wastewater at room temperature and results reported here are very promising.

* Corresponding author, e-mail: rajaryache@gmail.com, aryark@nitj.ac.in

Presented at the International Chemical Engineering Conference 2021 (ICHEEC): 100 Glorious Years of Chemical Engineering and Technology, held from September 16–19, 2021 at Dr B. R. Ambedkar National Institute of Technology, Jalandhar, Punjab, India.

2. MATERIAL AND METHODS

The basic red 9 (pararosaniline hydrochloride ($C_{19}H_{18}N_3Cl$), colour index: 42500, molecular weight: 323.9) dye was supplied by Merck, India. It was used as an adsorbate in the present study.

Cow dung ash, wheat straw, and saw dust were employed as adsorbents in preliminary research to determine the best adsorbent for the dye in consideration. For mixing, jar test apparatus (Scientific systems, New Delhi, India) and magnetic stirrer (Remi equipment pvt. Ltd., India) have been used. Colour analysis of samples was done using UV–VIS spectrophotometer (Model No. SL-159, Elico, India). The pH was measured using a digital pH meter (Model No. MK-VI, Toshniwal, India).

2.1. Preparation of cow dung ash adsorbent

Cow dung cake was collected and dried before being burned in open air. The ash was allowed to cool to room temperature before being placed in an airtight container. Then ash was pounded into a fine powder using a hand hammer, and the adsorbent was then divided into five distinct particle sizes using sieves of 60, 85, 100, 170, and 200 BSS mesh. For experimental uses, screened powder from various screens was collected and stored in airtight glass sample bottles.

2.2. Characterization of the adsorbent by scanning electron microscope (SEM)

A SEM was used to examine the adsorbent (ZEISS EVO Series Model: EVO15, supplied by Carl Zeiss India, Bangalore, India, Pvt Ltd). SEM pictures of cow dung ash at 1000, 10000, and 20000 magnifications are shown in Figures 1a–d. Figures 1a, 1b, and 1c show particles that appear to be flakes.Particles are found

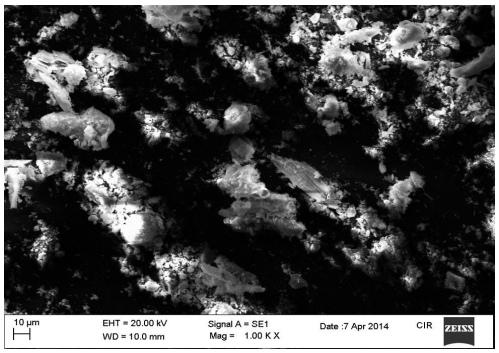

(a) SEM photographs of the cow dung ash at 1000 magnification

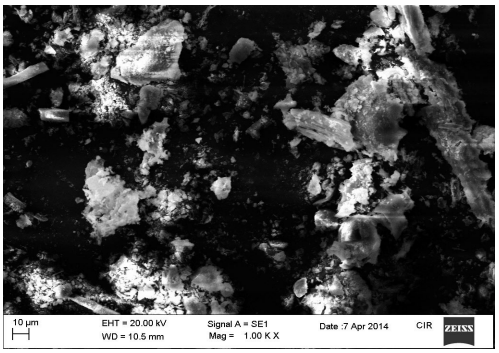

(b) SEM photographs of the cow dung ash at 1000 magnification at different location

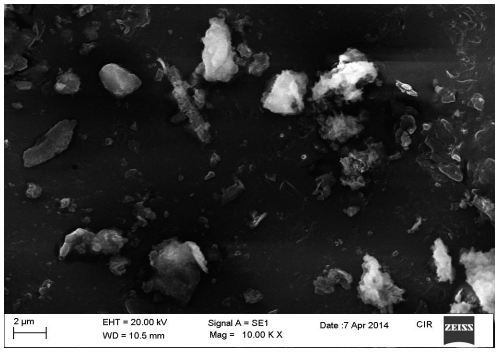

(c) SEM photographs of the cow dung ash in 2 micron size at 10000 magnification

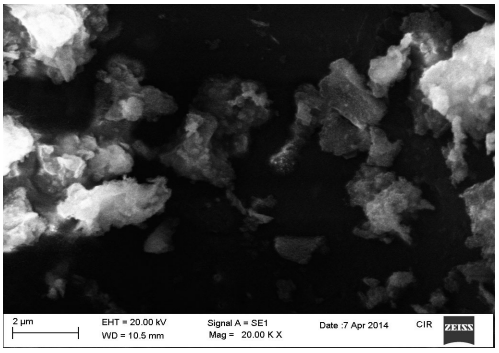

(d) SEM photographs of the cow dung ash in 2 micron size at 20000 magnification

Fig. 1. SEM photographs of the cow dung ash

as clusters of particles less than 1 micron in size, as seen in Figure 1d. At higher pH, these clusters may separate, resulting in increased efficiency.

2.3. Study of zero-point charge of cow dung ash adsorbent

The point of zero charge (pH_{ZPC}) of an adsorbent (cow dung ash) was determined by using five beakers in which solid to liquid ratio – 1:1000 was taken. A 0.5 gm adsorbent dosage of cow dung ash was applied to two litre glass beakers, each containing 500 ml of distilled water with a pH ranging from 2–10. 0.1N H_2SO_4 and 0.1N NaOH solutions were used to maintain pH of distilled water at 28 °C. Graph was plotted between initial and final pH of distilled water as in Figure 2. The pH_{ZPC} of cow dung ash was obtained at pH 8.8 which was used in the experiments.

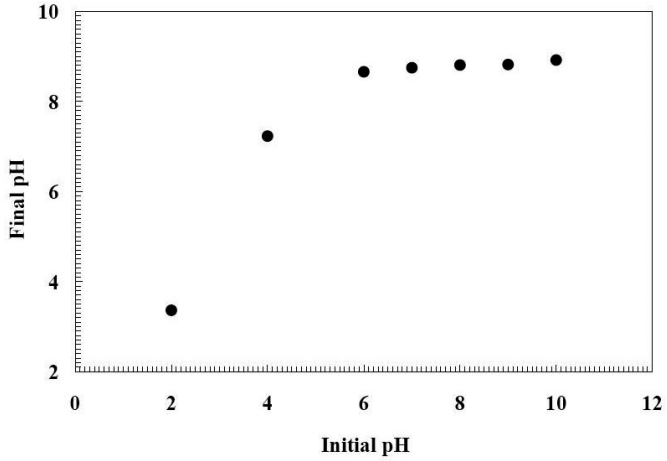

Fig. 2. Point of zero charge (pH_{ZPC}) of cow dung ash used for the adsorption; adsorbent dose: 0.5 gm/500 ml in each sample, agitation speed 300 rpm, agitation time 8 hrs

2.4. Calibration curve

A known quantity of dye was diluted in distilled water to make a stock solution (20 mg/L) for calibration curve, followed by production of solutions with various dye concentrations. Using jar test apparatus, each diluted solution was allowed to agitate for 30 min at 300 rpm at 30 °C. This dye's highest absorption wavelength is in the range of 540–540.1 nm. In the visible area, absorbance values for each sample of varied dye concentrations were recorded and plotted using UV–VIS spectrophotometer as in Figure 3.

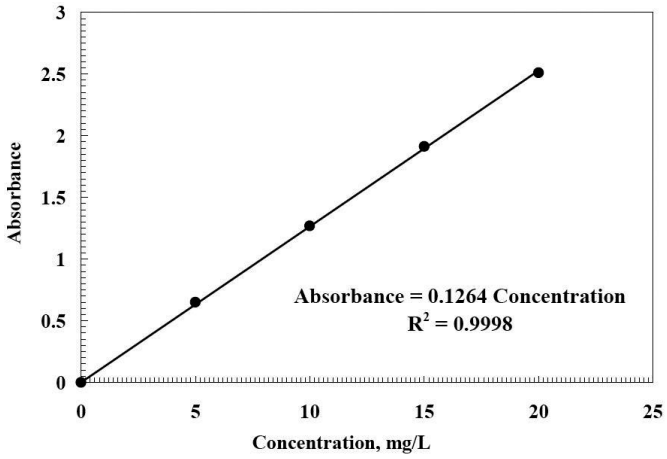

Fig. 3. Calibration curve for pararosaniline hydrochloride dye

2.5. Calculation of the amount of dye adsorbed

The sample was agitated using jar test apparatus at speed of 300 rpm for 3 h. Samples were taken at equilibrium from this solution with the help of dropper and poured on the Whitman filter No. 44 on the funnel to get adsorbent free solution for absorbance measurement. The dye concentration in the sample had been calculated using an earlier prepared calibration curve. The amount of dye adsorbed per gm adsorbent is calculated using the following equation.

$$q_t = \frac{C_0 - C_t}{M} \cdot V \tag{1}$$

where q_t – amount of dye adsorbed of adsorbent, mg/g, C_0 – initial dye concentration, mg/L, C_t – dye concentration, mg/L at time t, V – volume of solution, L, and M – mass of adsorbent, g.

Twelve solutions of basic red 9 dye with varying concentrations of 10, 20, 30, 40, 50, 60, 70, 80, 90, 100, 110, and 120 mg/L were prepared in two litre glass beakers with a solution volume of 500 ml in each beaker. To ensure sufficient mixing, a jar test apparatus was used to agitate mixture for 30 minutes at 300 rpm. Beakers were exposed to atmosphere, and it was ensured that no solution droplets escaped during agitation. UV-vis spectrophotometer was used to measure initial absorbance of each solution. 0.5 g of prepared cow dung ash adsorbent was added in different solutions and agitated all solutions for 3 h to achieve equilibrium. Then final absorbance of each solution were recorded as given in Table 1.

Table 1. Initial and final concentrations of different solutions

S. No.	Solution prepared, mg/L	Initial absorbance	Final absorbance	Initial concentration, C_o, mg/L	Final concentration, C_e, mg/L	Amount adsorbed, q_e, mg/g
1	10	1.669	0.124	13.90	1.033	12.867
2	20	3.29	0.236	27.416	1.966	25.45
3	30	4.577	0.334	38.142	2.783	35.359
4	40	5.806	0.529	48.383	4.408	43.975
5	50	6.134	0.649	51.116	5.408	45.708
6	60	6.596	0.800	54.916	6.666	48.250
7	70	7.032	1.051	58.600	8.758	49.842
8	80	7.269	1.206	60.575	10.050	50.525
9	90	7.686	1.376	64.050	11.466	52.584
10	100	7.927	1.495	66.058	12.458	53.60
11	110	8.019	1.536	66.825	12.800	54.025
12	120	8.112	1.599	67.600	13.325	54.275

3. RESULT AND DISCUSSION

3.1. Effect of contact time on dye removal

Experiments were conducted to assess how long it takes for adsorption system to attain equilibrium. A contact duration was longer than assigned to each run. Adsorption of dye was calculated after 5, 10, 20, 30, 40, 60 and 90 min contact times for samples containing four different initial dye concentrations

of 10, 20, 30, and 40 mg/L, adsorbent dose of 0.5 g was added into each 500 mL solution of dye having different concentrations at a temperature 25 °C and 8.5 pH. Figure 4 depicts the influence of initial dye concentration on adsorption rate. Due to surface mass transfer, the process was found to be quite fast at first, and a substantial portion of the entire amount of dye was eliminated in a few minutes.

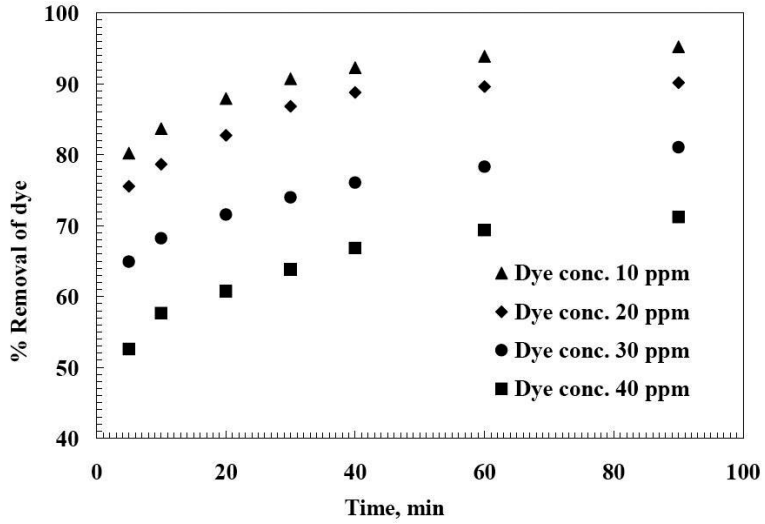

Fig. 4. Effect of contact time and dye concentration on percentage removal of dye

The dye adsorption was shown to be very efficient within first 5 min, with around 80% of dye being adsorbed in that time. In another 35 min, total amount of dye removed increased to 90%, which was only 10% increase over previous 35 min. It was noted that it took 40 min for cow dung ash to reach equilibrium. After this till 90 min, there was no major difference in dye removal. This reveals that cow dung ash was quick adsorbent for dye removal, and 40 min was enough time to remove 90% of the dye.

At low concentrations, cow dung ash was shown to be a more efficient adsorbent as % dye removal was great, as shown in Figure 4. The % of dye removed decreased as the initial concentration rose as dye adsorption depends on the number of available unoccupied sites on adsorbent's surface, and there were fewer active sites available at high dye concentrations.

3.2. Effect of adsorbent dose on dye removal

To evaluate effect of adsorbent dosage, three dye samples of 20, 30, and 40 mg/L were prepared. The adsorbent doses were changed from 0.5 to 2.0 gm with a 0.5 gm increment. The % dye adsorption increased as the adsorbent dosages were increased, as seen in Fig. 6 and in Table 2. The active surface area and number of adsorption sites fluctuate as adsorbent dosages were varied. As a result, increasing the adsorbent dose expanded available surface area and adsorption sites for dye adsorption, resulted in improved dye adsorption. Therefore, it was worth putting more dose in highly concentrated dye samples. When adsorbent dose was raised from 0.5 to 1.5 gm/L for dye samples with concentrations of 30 and 40 mg/L, % dye removal rose fast. In these samples, as dye removal was restricted, the amount of adsorbent addition was limited.

Figure 5 shows that with a fixed dye concentration, the dye uptake ratio (mg of dye/gm of adsorbent) declined when adsorbent dosage increased. At the same time, total removal efficiency notably improved. The dye absorption value was reduced due to splitting effect of flux-concentration gradient between adsorbate and adsorbent.

Table 2. Percentage dye removal at different adsorbent doses and different concentrations

Dye concentration, mg/L	% dye removal at different adsorbent doses			
	0.5 gm/L	1.0 gm/L	1.5 gm/L	2.0 gm/L
20	90	91	92	95
30	80	85	90	92
40	70	78	82	85

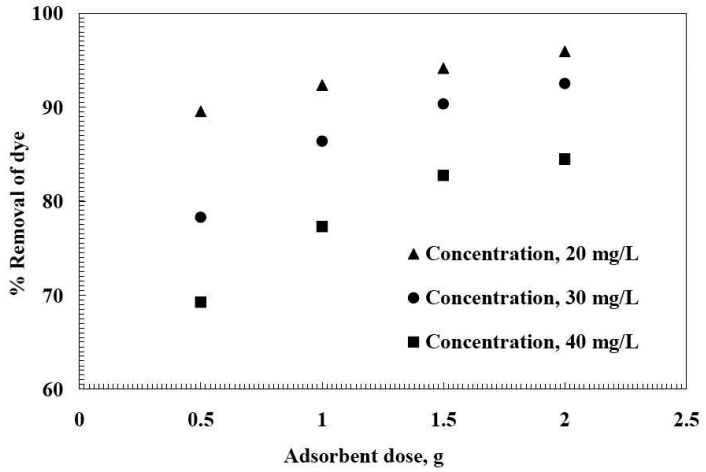

Fig. 5. Effect of adsorbent doses on the dye removal. Agitation speed, temperature and solution pH and batch time were 300 rpm, 25 °C, 8.5, and 90 min respectively

3.3. Effect of agitation speed on dye removal

In adsorption phenomena, the distribution of solute in the bulk solution and development of the outer boundary layer are both affected by agitation speed. Figure 6 illustrates proportion of dye removed with cow dung ash at various agitation speeds of 200, 300, and 400 rpm during a 90-minute period.

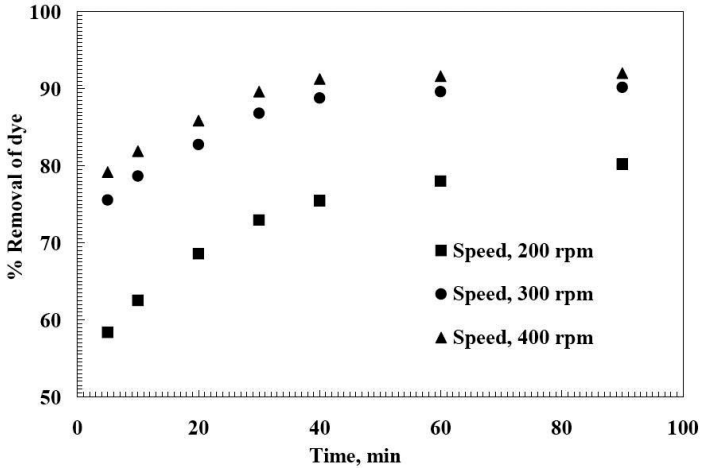

Fig. 6. Effect of agitation speed on the percentage adsorption of dye as a function of time, Initial dye concentration, adsorbent dose, temperatures and pH were 20 ppm, 1.0 gm/L, 25 °C, and pH 8.5 respectively

When agitation speed increased from 200 to 300 and 300 to 400 rpm, % of dye removed increased from 80.21 to 90.19% and 90.19 to 92.04%. Extending contact time to 24 hours did not notably improve dye

adsorption, and observed absorbance values were 0.0024, which is considered insignificant. The film boundary layer containing adsorbent particles reduced when the agitation speed was increased.

3.4. Effect of pH on dye removal

The pH of dye solution at its initial level controls dye solution's adsorption process. The pH of solution can be affected by adsorbent's surface charge, degree of ionisation of adsorbate, and level of dissociation of functional groups on active sites of adsorbent. The pH of dye solutions was changed from 2 to 10 by adding H_2SO_4 and NaOH to see if pH had an effect on degree of dye adsorption. Figure 7 shows % of dye removal at various pH values for initial dye concentration of 20 mg/L. Maximum adsorption occurs at a pH of 8.5 for the dye under consideration. The change in dye absorption dependent on original solution pH may be explained by structure of dye molecule and adsorbent's point of zero charge, pH_{ZPC}.

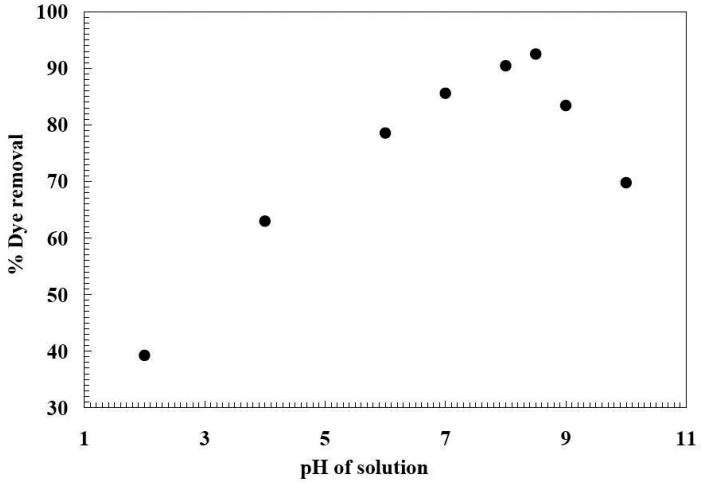

Fig. 7. Effect of pH on the percentage dye adsorption; adsorbent dose, and agitation speed were 1.0 gm/l, and 300 rpm respectively

The zero-charge point for cow dung ash was determined to be 8.8. An adsorbent particle collects more negatively charged species above this pH, and the surface tends to accrue negative charge, whilst adsorbate species in alkaline media stay positively charged. Two forces of attraction, electrostatic force and coulombic force, are key interactions that impact dye adsorption on adsorbent materials in this case. The electrostatic interaction between positively charged adsorbate species and negatively charged adsorbent particles would increase due to negatively charged absorbent surface, resulting in enhanced dye adsorption (Bhattacharya and Venkobachar, 1984). Production of soluble hydroxyl compounds between absorbent and dye caused a decrease in adsorption above pH 8.8. The adsorbent surface obtained more positively charged sites and dye molecules attained positive charge at a pH lower than pH_{ZPC}.

3.5. Effect of adsorbent particle size on dye removal

For sieving cow dung ash in five different particle sizes passing through 60, 85, 100, 170 and 200 BSS mesh were selected. Batch adsorption tests were carried out to different mesh sizes by shaking the same quantity of 0.5 g of cow dung ash adsorbent in each 500 mL of an aqueous solution of dye of specified concentration (20 mg/L). Figure 8 show that dye adsorption rose as mesh size increased and when particle size of the adsorbent dropped throughout saturation phase, the amount of dye adsorbed increased. As a consequence, reducing particle size or increasing mesh size improves dye adsorption capacity.

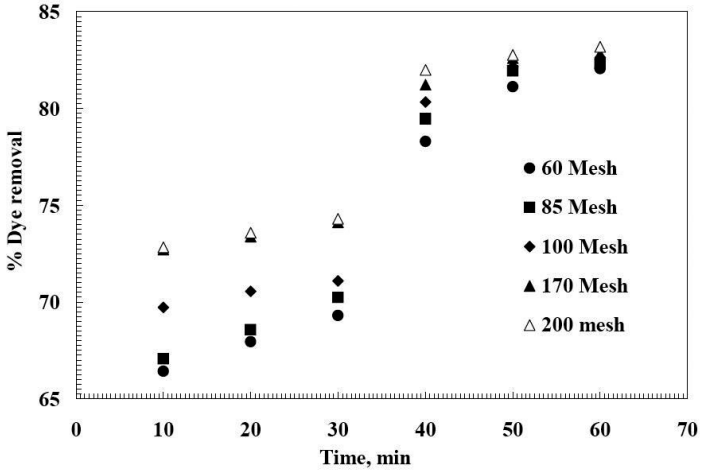

Fig. 8. Effect of adsorbent particle size on dye removal efficiency; adsorbent dose, agitation speed, and temperature were 20 mg/L, 8.5,1.0 g/L, 300 rpm, and 20 °C respectively

3.6. Adsorption equilibrium studies

It is common to express equilibrium data on the basis of an isotherm equation to implement it for predicting operating lines and design application (McKay et al., 1999). While the Freundlich isotherm had been successfully used to forecast adsorption equilibria for comparable systems (Nassar et al., 1995), Langmuir isotherm was explored to assess data, primarily because the equilibrium findings demonstrate a strong propensity to attain monolayer saturation capacity. The linear form of Langmuir isotherm model, which is based on assumption of monolayer coverage of the adsorbate at the adsorbent's outer surface Wang and Wang (2007) may be expressed as the following equation:

$$\frac{1}{q_e} = \frac{1}{q_m} + \frac{1}{K_L q_m C_e} \tag{2}$$

where, q_e – mg dye adsorbed per g adsorbent at equilibrium, q_m – amount of moles of solute adsorbed per unit of adsorbent weight in creating a complete monolayer on the surface, mg/g, C_e – concentration of dye remaining in solution at equilibrium, mg/L, K_L – Langmuir constant related to the energy or net enthalpy ΔH of adsorption and q_m – maximum adsorption capacity having units, L/mg and mg/g.

Multiplying Eq. (2) C_e will give the following equation

$$\frac{C_e}{q_e} = \frac{C_e}{q_m} + \frac{1}{K_L q_m} \tag{3}$$

The graph between C_e and $\frac{C_e}{q_m}$ is drawn, as depicted in Figure 9. The equation of best fit line with regression coefficient of 0.9986 is given by

$$\frac{C_e}{q_m} = 0.0161 C_e + 0.032 \tag{4}$$

The values of q_m and K_m have been calculated from slope and intercept of Eq. (4):

- $\frac{1}{q_m} = 0.0161 \rightarrow q_m = 62.118 \frac{\text{mg}}{\text{g}}$ and
- $\frac{1}{K_L q_m} = 0.032 \rightarrow \frac{0.0161}{K_L} = 0.032 \rightarrow K_L = 0.053 \frac{\text{L}}{\text{mg}}$.

The following adsorption isotherm models were fitted to the experimental data. For Freundlich isotherm model, the equation comes out to be

$$\ln q_e = 0.2416 C_e + 3.3813, \quad R^2 = 0.9423 \tag{5}$$

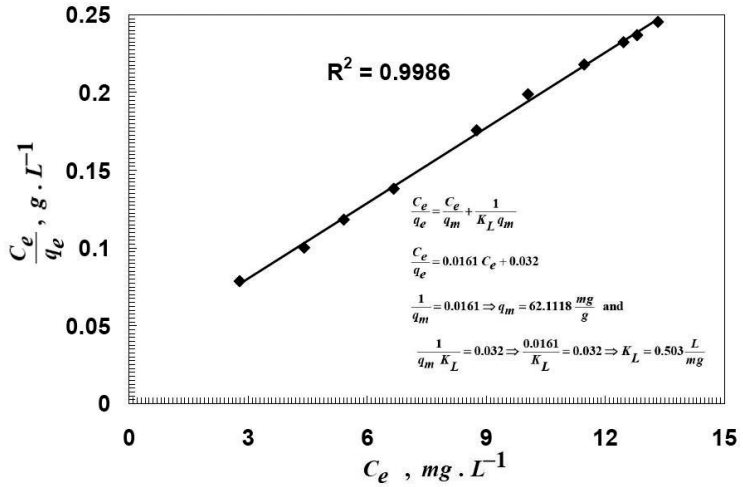

Fig. 9. Langmuir plot for the adsorption of dye by cow dung ash

Compared with Freundlich isotherm model, $\ln q_e = \frac{1}{n} \ln C_e + \ln K$, the values of n and K come out to be 4.1391 and 29.4089 respectively.

For Temkin isotherm model, the equation comes out to be

$$q_e = 10.944 \ln C_e + 26.192, \quad R^2 = 0.9668 \tag{6}$$

Compared with Temkn isotherm model, $q_e = \ln C_e$, the values of a and b come out to be 26.192 and 10.944 respectively. The data fits Langmuir isotherm model quite well as shown in graphs.

3.7. Adsorption kinetics

The adsorption kinetics had been studied using three different models: pseudo–first, pseudo–second order and simple Elovich kinetic models (El-Ashtoukhy et al., 2008). Lagergren first rate equation is most commonly used to study the adsorption of solute from liquid solution and the equation for this model is as follows (Jianlong et al., 2001):

$$\ln (q_e - q_t) = \ln q_e - K_{1ad} t \tag{7}$$

where q_e – mass solute adsorbed at equilibrium, mg/g, q_m – mass of solute adsorbed at time t, mg/g, and K_{1ad} – first-order reaction rate constant, l/min.

The pseudo–second order equation based on equilibrium adsorption capacity is given as

$$\frac{t}{q_e} = \frac{1}{K_{2ad} q_e^2} + \frac{t}{q_m} \tag{8}$$

where, q_e – equilibrium adsorption capacity, mg/g, t – time, min, and K_{2ad} – second order reaction rate equilibrium constant, g/(mg·min).

The simple Elovich model is given by, $q_t = \alpha + \beta \ln t$, where q_t is the mass of solute adsorbed at time t, mg/g. Figures 10–12 show adsorption kinetic curves at different dye concentrations for the same adsorbent and other parameters. For all models, data were fitted to straight-line fitting and equations for each and every case with other parameters as depicted in Table 3. The data fit well for pseudo–second order model for which linear regression coefficient, $R^2 \geq 0.9991$.

Table 3. Comparison of various adsorption kinetics model studies

Dye concentration, ppm	Pseudo-first order $\ln(q_e - q_t) = \ln q_e - K_{1ad}t$			Pseudo-second order $\frac{t}{q_e} = \frac{1}{K_{2ad}q_e^2} + \frac{t}{q_m}$			Simple Elovich model $q_t = \alpha + \beta \ln t$			
	Equation	K_{1ad}, l/min	R^2	Equation	K_{2ad}, g/(mg·min)	R^2	Equation	α	β	R^2
10	$\ln(q_e - q_t) = 3.0802 - 0.0044t$	0.0044	0.8805	$\frac{t}{q_e} = 0.1688 + 0.1035t$	0.0634	0.9999	$q_t = 16.815 + 2.6183 \ln t$	16.815	2.6183	0.9918
20	$\ln(q_e - q_t) = 2.2740 - 0.0038t$	0.0038	0.7552	$\frac{t}{q_e} = 0.086 + 0.0545t$	0.0345	0.9999	$q_t = 16.628 + 1.6751 \ln t$	16.628	1.6751	0.9943
30	$\ln(q_e - q_t) = 1.5157 - 0.0041t$	0.0041	0.8226	$\frac{t}{q_e} = 0.104 + 0.0404t$	0.0156	0.9991	$q_t = 13.316 + 1.1185 \ln t$	13.316	1.1185	0.9629
40	$\ln(q_e - q_t) = 2.7457 - 0.0040t$	0.0040	0.9227	$\frac{t}{q_e} = 0.1117 + 0.034t$	0.0104	0.9991	$q_t = 7.1637 + 0.5425 \ln t$	7.1637	0.5425	0.9908

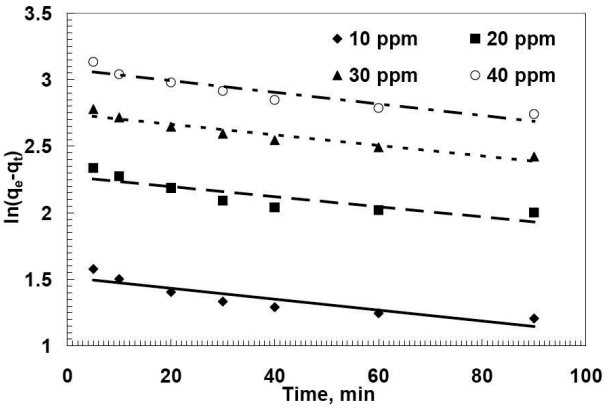

Fig. 10. Pseudo-first order adsorption kinetics for adsorption of basic red 9 dye on cow dung ash

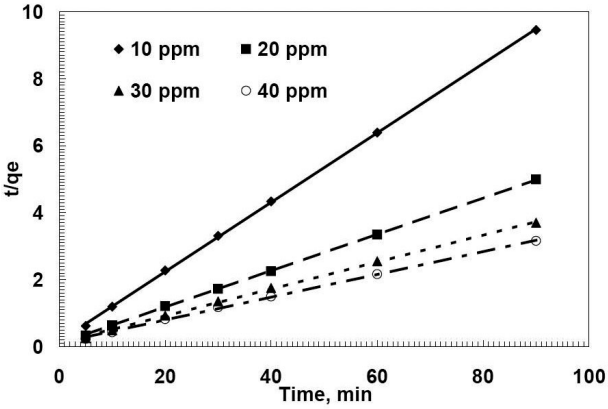

Fig. 11. Pseudo–second order adsorption kinetics for adsorption of basic red 9 dye on cow dung ash

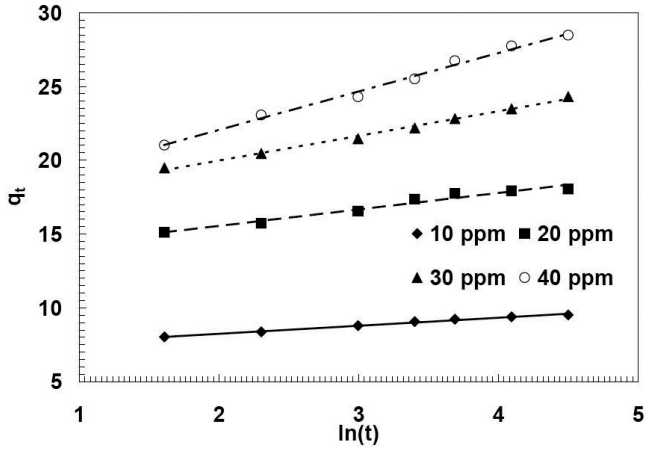

Fig. 12. Simple Elovich adsorption kinetics for adsorption of basic red 9 dye on cow dung ash

3.8. Macro and micro-pore diffusion

The three primary processes in the adsorption process are film diffusion, pore diffusion, and intra–particle transport, respectively. The intra–particle diffusion model is given below (El-Ashtoukhy et al., 2008).

$$q_t = K_{id} t^{\frac{1}{2}} + I \tag{9}$$

where, K_{id} is the intra–particle diffusion rate constant, mg/(g·min$^{1/2}$). Figure 13 presents the intra–particle diffusion curve for adsorption at different dye concentrations. The straight line fitting was done using two sections (El-Ashtoukhy et al., 2008; Ramaraju et al., 2014). Table 4 shows the straight-line equations for each section, $K_{id,1}$, $K_{id,2}$, I_1, I_2, and R^2. The larger values intercept, I, signifies that boundary layer is affecting the adsorption. Sarkar et al. (2003) found that the first portion of Figure 13 indicates boundary layer effects and second portion indicates intra–particle/or pore diffusion, and third portion indicates the final equilibrium stage (Cheung et al., 2007). However, in the present study only two sections have been observed for the dye and adsorbent under consideration. The first and second portions of Figure 13 show the bulk diffusion and intra–particle diffusion, respectively Allen et al. (1989). Because of the low solute concentration, intra–particle diffusion slowed down when the equilibrium stage was achieved (Cheung et al., 2007; Ramaraju et al., 2014).

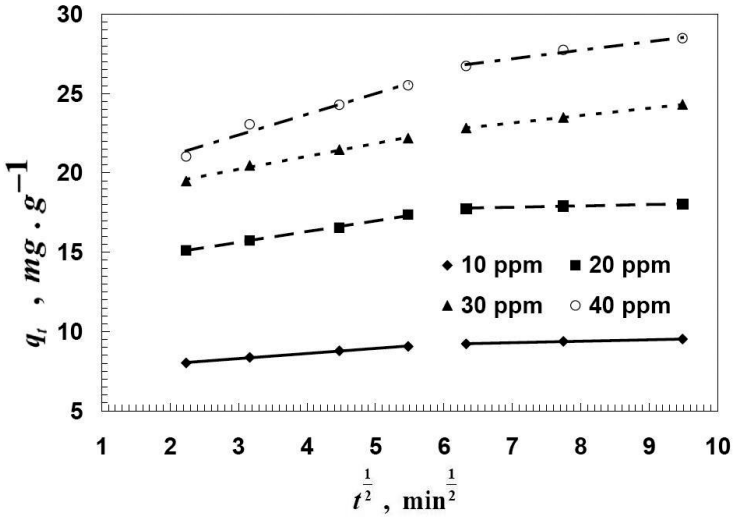

Fig. 13. Intra–particle diffusion plot for adsorption

The slopes of the straight lines correspond to the rate of adsorption. The slope of the first section is greater than the slope of the second section which indicates faster uptake in the initial phase and then it slows down. In the beginning, adsorbate is first delivered to macropores and mesopores, then slowly diffuses into micropores, as described earlier Kumar et al. (2003). The displacement of the straight lines from the origin represents the difference between the initial and final mass transfer rates of adsorption (Poots et al., 1978). Straight line deviations from the origin also imply that pore diffusion is not the primary rate regulator.

Table 4. Kinetic parameters for diffusion model

Section 1				
Dye concentration, ppm	Equation	$K_{id,1}$ mg/(g·min$^{1/2}$)	I_1	R^2
10	$q_t = 0.3229t^{\frac{1}{2}} + 7.3262$	0.3229	7.3262	0.9966
20	$q_t = 0.6858t^{\frac{1}{2}} + 13.5580$	0.6858	13.558	0.9971
30	$q_t = 0.8264t^{\frac{1}{2}} + 17.7290$	0.8264	17.729	0.993
40	$q_t = 1.3205t^{\frac{1}{2}} + 18.4080$	1.3205	18.4080	0.968
Section 2				
Dye concentration, ppm	Equation	$K_{id,2}$ mg/(g·min$^{1/2}$)	I_2	R^2
10	$q_t = 0.0924t^{\frac{1}{2}} + 8.6554$	0.0924	8.6554	0.9889
20	$q_t = 0.0877t^{\frac{1}{2}} + 17.2180$	0.0877	17.218	0.9730
30	$q_t = 0.4735t^{\frac{1}{2}} + 19.8280$	0.4735	19.8280	1.0000
40	$q_t = 0.5454t^{\frac{1}{2}} + 23.369$	0.5454	23.3690	0.9778

4. CONCLUSSIONS

Cow dung is a common waste product that has been transformed into a low-cost adsorbent material. The adsorbent prepared from cow dung exhibits very good adsorption capacity. It has shown the excellent performance for the removal of Basic red 9 as compared to other low cost adsorbent like sunflower stalks which takes 30 minutes to remove 80% dye (Sun and Xu, 1997). Percentage dye removal was 80.24% and 95.24 in 5 minutes and 90 minutes, respectively, at initial dye concentration of 10 ppm. Hence, the developed adsorbent may be a good alternate as compared to commercially available adsorbents for dye removal because of its comparable efficiency and a significantly low cost. The findings of this study might be used to the design of a dye-rich industrial wastewater treatment facility in the future.

The authors are highly grateful to Department of Chemical Engineering, Jaypee University of Engineering and Technology, Guna for providing necessary infrastructure to conduct the experiment and Department of Chemical Engineering, Dr. B.R. Ambedkar National Institute of Technology, Jalandhar, for support to complete the research.

REFERENCES

Allen S.J., McKay G., Khader K.Y., 1989. Intraparticle diffusion of a basic dye during adsorption onto sphagnum peat. *Environ. Pollut.,* 56, 39–50. DOI: 10.1016/0269-7491(89)90120-6.

Bhattacharya A.K., Venkobachar C., 1984. Removal of cadmium (II) by low cost adsorbents. *J. Environ. Eng.,* 110, 110–122. DOI: 10.1061/(ASCE)0733-9372(1984)110:1(110).

Cheung W.H., Szeto Y.S., McKay G., 2007. Intraparticle diffusion processes during acid dye adsorption onto chitosan. *Bioresour. Technol.*, 98, 2897–2904. DOI: 10.1016/j.biortech.2006.09.045.

El-Ashtoukhy E.-S.Z., Amin N.K., Abdelwahab O., 2008. Removal of lead (II) and copper (II) from aqueous solution using pomegranate peel as a new adsorbent. *Desalination*, 223, 162–173. DOI: 10.1016/j.desal.2007.01.206.

Jianlong W., Xinmin Z., Decai D., Ding Z., 2001. Bioadsorption of lead(II) from aqueous solution by fungal biomass of *Aspergillus niger*. *J. Biotechnol.*, 87, 273–277. DOI: 10.1016/s0168-1656(00)00379-5.

Kumar A., Kumar S., Kumar S., 2003. Adsorption of resorcinol and catechol on granular activated carbon: Equilibrium and kinetics. *Carbon*, 41, 3015–3025. DOI: 10.1016/S0008-6223(03)00431-7.

McKay G., Porter J.F., Prasad G.R., 1999. The removal of dye colours from aqueous solutions by adsorption on low-cost materials. *Water Air Soil Pollut.*, 114, 423–438. DOI: 10.1023/A:1005197308228.

Nassar M.M., Hamoda M.F., Radwan G.H., 1995. Adsorption equilibria of basic dyestuff onto palm-fruit bunch particles. *Water Sci. Technol.*, 32, 27–32. DOI: 10.1016/0273-1223(96)00114-X.

Poots V.J.P., McKay G., Healy J.J., 1978. Removal of basic dye from effluent using wood as an adsorbent. *J. Water Pollut. Control Fed.*, 50, 926–935.

Ramaraju B., Reddy P.M.K., Subrahmanyam C., 2014. Low cost adsorbents from agricultural waste for removal of dyes. *Environ. Prog. Sustainable Energy*, 33, 38–46. DOI: 10.1002/ep.11742.

Sarkar M., Acharya P.K., Bhattacharya B., 2003. Modeling the adsorption kinetics of some priority organic pollutants in water from diffusion and activation energy parameters. *J. Colloid Interface Sci.*, 266, 28–32. DOI: 10.1016/S0021-9797(03)00551-4.

Sivarajasekar N., Baskar R., 2014. Adsorption of basic red 9 onto activated carbon derived from immature cotton seeds: isotherm studies and error analysis. *Desalin. Water Treat.*, 52, 7743–7765. DOI: 10.1080/19443994.2013.834518.

Sun G., Xu X., 1997. Sunflower stalks as adsorbents for color removal from textile wastewater. *Ind. Eng. Chem. Res.*, 36, 808–812. DOI: 10.1021/ie9603833.

Wang L., Wang A., 2007. Adsorption characteristics of Congo Red onto the chitosan/montmorillonite nanocomposite. *J. Hazard. Mater.*, 147, 979–985. DOI: 10.1016/j.jhazmat.2007.01.145.

Received 16 February 2022
Received in revised form 22 March 2022
Accepted 6 April 2022